https://ntrs.nasa.gov/search.jsp?R=19700002953 2018-07-24T00:06:11+00:00Z

U. of Iowa 69-46

Distribution of this document is unlimited.

N70-12257
NASA CR-106912

ELECTRON OBSERVATIONS BETWEEN THE INNER EDGE OF THE PLASMA SHEET AND THE PLASMASPHERE*

by

M. A. Schield and L. A. Frank

CASE FILE COPY

Department of Physics and Astronomy
THE UNIVERSITY OF IOWA
Iowa City, Iowa

U. of Iowa 69-46

ELECTRON OBSERVATIONS BETWEEN THE INNER EDGE OF THE PLASMA SHEET AND THE PLASMASPHERE*

by

M. A. Schield and L. A. Frank

August, 1969

Department of Physics and Astronomy
University of Iowa
Iowa City, Iowa 52240

NGL-16-001-002

*This research was supported in part by the National Aeronautics and Space Administration under grant NSG-233-62 and contract NAS5-2054 and by the Office of Naval Research under contract Nonr-1509(06).

Distribution of this document is unlimited.

U. of Iowa 69-46

Errata

ELECTRON OBSERVATIONS BETWEEN THE INNER EDGE OF THE PLASMA SHEET AND THE PLASMASPHERE by M. A. Schield and L. A. Frank

Page 1, line 18 should read:

was about half an earth radius closer to the earth than the 5 keV near-

Page 7, line 6 should read:

the electron intensities between 90 eV and 750 eV made a negligible

Page 20, line 3 should read:

inner edge at $\lambda \simeq 15°$ near local midnight could map onto an equatorial

Page 24, add to end of page:

Vasyliunas, V. M., Observations of low energy electrons with the OGO-A satellite, Ph.D. Thesis, M.I.T., 1966.

Vasyliunas, V. M., A survey of low-energy electrons in the evening sector of the magnetosphere with OGO 1 and OGO 3, J. Geophys. Res., 73, 2839, 1968.

Abstract

Electron observations between ~ 100 eV and 50 eV are presented for L values between 3 and 10 R_E (R_E, earth radii) near local midnight at low magnetic latitudes. These measurements were obtained between June 9 and July 23, 1966, with electrostatic analyzers borne on OGO-3. The inner edge of the plasma sheet is characterized by a sudden exponential decrease in the electron energy density. This near-earth decrease has a very distinct structure with fluxes of higher energy electrons decreasing further from the earth for electron energies between 750 eV and 20 keV. A trough of ~ 100 eV electrons with densities of ~ 1 $(cm)^{-3}$ is observed to fill the region between the inner edge of the plasma sheet and the plasmasphere. The density of electrons above 750 eV is often less than 0.1 $(cm)^{-3}$ in this region. The separation between the inner edge of the plasma sheet and the plasmapause was between 1 and 3 R_E in June and increased to between 3 and 5 R_E in July. Analysis of subsequent data should determine whether this is a latitude or local time effect. The plasmapause is commonly located at the minimum of the energy density profile for electron energies above 750 eV. A plasmapause structure consisting of a sharp outer edge and a broad inner edge is observed mainly in the 200 eV electron fluxes. Observed lifetimes of ~ 10 days for lower-energy electrons (E ~ 1 keV) within the plasma-

sphere are in agreement with lifetimes for more energetic electrons ($E \geq 500$ keV) in the same region. Kilovolt electrons between the plasmasphere and the inner edge of the plasma sheet are removed within the satellite's orbital period of 48 hours. Differential energy spectrums of electron intensities for the plasma sheet, the inner edge, the electron trough and the plasmasphere are presented.

I. Introduction

The plasma sheet is by its location and nature central to the origin of both the aurora and ring currents. And although the plasma sheet was first observed about ten years ago, experimental design problems have until recently hindered the acquisition of accurate and comprehensive measurements concerning its nature (cf Gringauz [1969] and Frank [1967a,b] and the references therin for a review of low energy plasmas within the magnetosphere). Vasyliunas [1968] observed that the plasma sheet had a 'well-defined sharp inner-boundary'. Between 1700 and 2100 LT (geocentric local time) this inner boundary was located at 11 ± 1 R_E (R_E, earth radii) during geomagnetically quiet periods. Characteristically the electron energy density decreased exponentially inward with a scale length of about 0.4 R_E while the number density remained essentially constant across the inner edge of the plasma sheet. During magnetic storms of the bay type the inner boundary moved inward to between 6 and 8 R_E. Frank [1967d, 1968] observed that this near-earth decrease occurred at increasing radial distances for higher energy electrons between 1 and 10 keV. The 2 keV near-earth decrease was about half an earth radii closer to the earth than the 5 keV near-earth decrease. No general relationship was observed between the location of this near-earth decrease and the boundary of trapping for higher

energy ($E \gtrsim 50$ keV) electrons. The purpose of this paper is to examine the region between the inner edge of the plasma sheet and the plasmasphere in detail. Only electron data acquired at low magnetic latitudes near local midnight are presented.

II. Orbit and Instrumentation

OGO-3 was launched on June 7, 1966 into a highly eccentric orbit with an apogee of ~ 20 R_E, an inclination of 30°, a period of ~ 48 hours and with the line of apsides directed to ~ 22:00 LT. An attitude system provided a predetermined, monitored spacecraft orientation. All data presented here were acquired before the electrical failure of the attitude system on July 23, 1966. Figure 1 illustrates several representative inbound passes as functions of magnetic latitude and local time. Local times between 21:20 and 01:20 were covered on these inbound passes from 10 to 5 R_E during this period.

The University of Iowa instrumentation utilizes four Bendix Channeltrons and four cylindrical-plate electrostatic analyzers. The analyzers were paired in order to measure simultaneously and separately the differential energy spectrums of proton and electron intensities with an energy range extending from ~ 100 eV to ~ 50 keV. These two pairs of Low Energy Proton and Electron Differential Energy Analyzers designated LEPEDEA's A and B had orthogonal fields of view. The fields-of-view for LEPEDEA A were directed earthward and those for LEPEDEA B were directed perpendicular to LEPEDEA A's fields-of-view in the satellite-earth-sun plane. See Frank [1967a] and the references therein for additional details concerning instrumentation.

Energy bandpasses for the electron channels are shown in Table I. The analyzer plate voltages were stepped every 19 seconds and the corresponding channels were sampled at least 15 times per step. A complete spectrum including all 15 channels was acquired in approximately 5 minutes.

TABLE I

Energy Bandpasses for OGO-3 LEPEDEA

Electron Channels 'A' and 'B'

Electron Channel	Energy Bandpasses 'A'	'B'
3	90 - 160 eV	80 - 140 eV
4	190 - 330 eV	170 - 300 eV
5	310 - 540 eV	280 - 500 eV
6	410 - 720 eV	380 - 680 eV
7	640 -1100 eV	610 -1100 eV
8	.99 - 1.7 keV	.94 - 1.7 keV
9	1.5 - 2.7 keV	1.5 - 2.7 keV
10	2.6 - 4.6 keV	2.8 - 5.0 keV
11	3.8 - 6.8 keV	4.1 - 7.2 keV
12	6.8 - 12 keV	5.8 - 10 keV
13	10 - 18 keV	9.8 - 17 keV
14	14 - 24 keV	14 - 24 keV
15	27 - 47 keV	26 - 46 keV

III. Observations

In the first two sections electron measurements for several inbound passes are presented and analyzed. Observational periods on June 23, and July 17 and 19, 1966 were chosen to represent those of typical inbound passes during quiet conditions. In subsequent sections data from other inbound passes are utilized to evaluate the main features observed in these measurements.

June 23, 1966. OGO-3 was inbound within one hour of local midnight at low magnetic latitudes as L decreased from 8 to 4 R_E. Figure 2 illustrates the differential electron intensities across the inner edge of the plasma sheet and into the plasmasphere. Initially the higher energy fluxes (tens of keV) decreased while the keV fluxes remained constant. Within a geocentric radial distance of 0.5 R_E the lower energy fluxes ($E \sim 1$ keV) also began to decrease and the peak flux shifted from channel 8 to channel 7. Within 1 R_E the higher energy fluxes began to stabilize while the lower energy continued to decrease. Simultaneously significant electron fluxes with $E \sim 100$ eV were first observed. Within 1.5 R_E the plasmapause was encountered at 06:22. Inside the plasmasphere the differential intensities between 100 eV and 50 keV increased smoothly and simultaneously as the radius decreased.

Figure 3 illustrates the radial dependence of the electron energy and number density corresponding to the fluxes illustrated in Figure 2. Above 750 eV the electron energy density decreased by a factor of 20 across the inner edge of the plasma sheet while the number density decreased by about an order of magnitude. Although the electron intensities between 90 eV and 750 eV made a megligible contribution to the energy density, they were sufficiently large to maintain an essentially constant number density outside the plasmasphere. The region between the inner edge of the plasma sheet and the plasmapause containing electrons with energies of $\sim$ 100 eV and densities of $\sim 1\ (\mathrm{cm})^{-3}$ will be denoted as the 'electron trough'. As such, this region is definitely a part of (but not necessarily identical with) Carpenter's [1966] 'plasma trough'. At the plasmapause both the number density and energy density increased abruptly. See the discussion of Figure 5 for further details.

Figure 4 illustrates the radial dependence of the differential spectrums of electron intensities for the measurements summarized in Figures 2 and 3. In the plasma sheet these electron spectrums are quite flat between 1 and 6 keV and then fall off rapidly. If the directional, differential intensities, dJ/dE, are fitted to an E^{-n} energy dependence, n is $\simeq .5$ between 1 and 6 keV and then softens to $\simeq 2.7$ between 6 and 20 keV. Across the inner edge of the plasma sheet

the higher energy fluxes decrease initially (spectrum 2a) and then the keV fluxes decrease while the 100 eV fluxes appear (spectrum 2b). Inside the plasmasphere the differential intensities are fairly smooth with $n \simeq 1.5$ between 300 eV and 50 keV (spectrum 3b). Below 300 eV the spectrum is quite soft with $n \simeq 3.5$. The energy and particle fluxes for these spectrums are summarized in Table II.

Figure 5 indicates that for electron intensities above 90 eV the plasmapause has a broad inner edge as well as a sharp outer edge. The outer edge has a scale of tens of kilometers. This is indicated by the factor of three increase in counting rate for channel 4A in less than five seconds at 6:22:18. The thickness of this outer edge would be about 15 km assuming the plasmapause velocity is much less than the satellite's radial velocity of about 4 $km(sec)^{-1}$. Fifteen km is the cyclotron radius for a 200-eV proton in the equatorial dipole field at 5.8 R_E.

The inner edge of the plasmapause has a scale of hundreds of kilometers and is displayed in Figures 2, 3 and 4. This structure is illustrated in Figure 5 by the shaded area in both frames. Within the plasmapause the electron fluxes between 90 and 750 eV decrease earthward. This inner edge has a thickness of between 200 km (based on the decay rate of the channel 5A responses within the 06:22 frame) and 1200 km (based on the decay rate of the channel 5A responses by

TABLE II

Electron Energy and Particle Fluxes

OGO 3; Inbound; 23 June 1966

$90\ eV \leq E \leq 50\ keV$

Spectrum	L, earth radii	Φ_E, ergs$(cm^2\text{-sec-sr})^{-1}$	J_e, $(cm^2\text{-sec-sr})^{-1}$
1a	8.2	5.6	6.3×10^8
1b	7.1	7.5	8.5×10^8
2a	6.4	1.8	4.5×10^8
2b	6.0	.66	1.9×10^8
3a	5.8	.62-.64	$4.-6. \times 10^8$
3b	5.6	.49	2.4×10^8

the 06:27 frame). Even if the plasmapause were moving with a constant velocity the ratio of the thickness of the inner and outer edges should be invariant. This ratio is between 20 and 120, which brackets the ratio of the cyclotron radii for protons and electrons with equal energies.

July 19-21, 1966. OGO-3 was inbound near the magnetic equator at about 22:00 LT for $L \simeq 9$. Figure 6 illustrates the electron number and energy density, and average energy across the inner edge of the plasma sheet and into the plasmasphere. Unlike the June 23 pass the inner edge of the plasma sheet is located several earth radii beyond the plasmapause and the electron trough begins at $L \simeq 9.5\ R_E$. On July 21 at 1300 U.T. at $L \leq 7$ substorm-related phenomena were observed. At $L \leq 8\ R_E$ the July 19 measurements closely resemble the July 21 pre-substorm measurements and are included in Figure 6. Above 90 eV the electron trough merges smoothly into the plasmasphere at $L \simeq 5.65\ R_E$. The electron trough is easily identified by the sudden decrease in the average energy from ~ 2-5 keV to ~ 50-80 eV due to the rapid decrease in the energy density versus a relatively constant number density.

Figure 7 illustrates electron spectrums characteristic of four electron regions within the magnetosphere: plasma sheet, inner edge, electron trough and plasmasphere. The inner edge spectrum illustrates characteristics of both the plasma sheet spectrum and of the electron trough spectrum. Although the electron trough spectrum somewhat

resembles the plasmasphere spectrum there are significant differences. Below 300 eV the electron-trough spectrum ($n \simeq 2$) is somewhat harder than the plasmasphere spectrum ($n \simeq 3$). Furthermore the electron trough spectrum should peak near ~ 100 eV while the plasmasphere spectrum should peak at ≤ 30 eV in order to produce the observed total electron densities of ~ 1 e/cm^3 and ~ 100 e/cm^3 in the respective regions [Carpenter, 1966]. During this pass the electron trough intensities increased steadily until at the plasmapause they matched the plasmasphere electron intensities at $L = 5.3\ R_E$. Normally there is an abrupt increase in the number density above 90 eV at the plasmapause.

In the following sections the remainder of the observations will be utilized to evaluate the electron observations of the plasmapause, the location and structure of the inner edge of the plasma sheet and the relationship with magnetic activity and local time.

Plasmapause Identification. A comparison of the plasmapause locations utilizing proton and electron data is illustrated in Table III. The proton plasmapause observations are based on the measurements by Taylor et. al., [1968] of ambient thermal ions between 1 and 45 atomic mass units using a radio-frequency ion spectrometer. The electron identification of the plasmapause is most easily made by identifying the localized enhancement of the 200 eV fluxes in channel 4A. During

TABLE III

Comparison of Plasmapause Locations

OGO-3; Inbound; 1966

DATE	PROTONS[a] (Ion Detector)		ELECTRONS (LEPEDEA)		DIFFERENCE	
	Time, U.T.	L, R_E	Time, U.T.	L, R_E	ΔT minutes	ΔL, R_E
11 June	02:20	7.04	~ 2:20	7.0	0	0
15 June	04:08	5.79	data gap		—	—
17 June	04:44	5.76	~ 04:47	5.6	~ 3	.15
19 June	04:54	6.70	~ 05:00	6.4	~ 6	.3
21 June	——	——	05:54	5.7	—	—
23 June	06:20	5.91	06:22	5.9	2	0
25 June	07:46	3.73	07:48	3.6	2	0
27 June	07:24	5.91	07:27	5.9	3	0
29 June	07:49	6.19	~ 07:53	6.0	~ 4	.2
1 July	09:01	4.76	~ 09:02	4.7	~ 1	0
3 July	08:45	6.44	~ 08:54	6.2	~ 9	.25
5 July	09:54	5.24	~ 09:53	5.2	~ 1	0
7 July	——	——	unidentifiable[b]		—	—
9 July	11:56	3.31	" "	"	—	—
11 July	11:55	4.62	" "	"	—	—
13 July	11:39	6.20	" "	"	—	—
15 July	——	——	~ 12:45	5.3	—	—
17 July	13:10	5.63	~ 13:10	5.6	0	0
19 July	13:44	5.64	~ 13:44	5.6	0	0
21 July	14:32	5.18	missing frame		—	—
23 July	14:46	5.78	unidentifiable		—	—

a. H. A. Taylor, Personal Communication, March 1969.
b. Intense fluxes above 700 eV precluded a decisive observation.

the July 9 storm, scattering from intense kilovolt fluxes masked this identification. Electron and proton observations of the plasmapause are normally within the five minute cycle time of the LEPEDEA experiment.

Structure and Location of the Inner Edge. Figure 8 summarizes the inbound profiles of the electron energy density between L = 10 R_E and the plasmapause as a function of L. The tendency for the lower energy fluxes to decrease closer to the earth is illustrated by the relative earthward displacement of the flux 'bar' for the lower energy channel. This tendency is clearly seen on every non-storm pass. Thus the structure illustrated in Figure 2 is a basic characteristic of the inner edge of the plasma sheet.

The location of the inner edge of the plasma sheet relative to the plasmapause is considerably different in July than in June for magnetically quiet days. In June the separation between the plasmapause and the inner edge of the plasma sheet is $\sim 1.5\ R_E$. In July this separation increases to $\sim 3\text{-}5\ R_E$ as the inner edge of the plasma sheet withdraws to $\sim 8.6\ R_E$. This change could be a latitude effect owing to the distortion of the earth's dipole field or a local time effect. Further analysis of the remaining OGO-3 data should clarify this point. During both June and July the plasmapause was often located at the minimum in the electron energy density profile.

Relation of Magnetic Activity. On June 25 the plasma sheet was first encountered at $L \simeq 9.3\ R_E$ at $\lambda \simeq 20°$. The plasma sheet electrons penetrated to $4\ R_E$ with a peak energy density of $\sim 3 \times 10^{-8}$ ergs$(cm)^{-3}$ and a number density of $\sim$ 10-30 $(cm)^{-3}$ above 90 eV. Within the plasmasphere this enhanced energy density decayed slowly with a lifetime of $\sim$ 10 days. On July 7 the inner edge of the plasma sheet withdrew to $L \simeq 9\ R_E$ and the plasmapause was not readily identifiable in either the electron or ion measurements.

The storm of July 9 is clearly indicated by both the location and magnitude of the electron energy-density peak. This storm has been analyzed in detail by Frank [1967c]. On July 9 the electron energy of 5×10^{21} ergs was about a fourth the proton energy of 21×10^{21} ergs for $1 \leq L \leq 8$. These proton and electron energy reservoirs were shown to be capable of explaining the observed decrease of $\sim 70\gamma$ at the earth's surface.

Unlike the protons which have charge-exchange lifetimes of about a day at $L = 4$ [Swisher and Frank, 1968] the electron peak persists with a lifetime of $\sim$ 10 days. Thus the lifetime of low energy electrons ($1 \leq E \leq 50$ keV) appears to be similar to the lifetime of high-energy electrons ($E \geq 500$ keV) in the same regions [Roberts, 1969]. Outside the plasmapause the enhanced electron energy densities are quickly dissipated within 2 days.

On July 21 the inner edge of the plasma sheet was encountered at $L = 9.7\ R_E$. At 13:00 U.T. a substorm began at College, Alaska, which had just moved through the premidnight sector. One hour later the electron energy-density increased by a factor of four near $L = 6\ R_E$. If this was indeed a second encounter with the inner edge of the plasma sheet, its inward radial velocity must have exceeded 5.5 km/sec during that hour. An electric field of $\sim .6$ mv/m would drift plasma at this velocity in a 100γ field. Further analysis of the proton population will be necessary to interpret the substorm behavior.

IV. Discussion

Structure of the Inner Edge. The simplest explanation for the existence of an inner edge to the plasma sheet would be that the electrons were being drifted across a retarding potential $\Delta\Phi$. Assuming a uniform magnetic field the general features of this model would be:

(1) the high energy tail ($E > e\Delta\Phi$) of the electron spectrum would remain unchanged across the potential,

(2) the integral flux, energy flux and energy density should all decrease earthward,

(3) for a peaked differential-energy spectrum, both the energy and magnitude of the peak intensity should decrease earthward.

This simple model is inadequate to explain the transistion from the plasma sheet spectrum 1b (Figure 4) to the spectrum of the inner edge of the plasma sheet 2b. Between spectra 1b and 2a the energy of the peak flux decreases by about 500 eV. Yet the fluxes above 4 keV have decreased considerably while the peak flux has actually increased. Between 2a and 2b, the first two criteria are satisfied but there is not an accompanying decrease in the energy of the peak flux. Beyond 2b the total flux, energy density and number density all increase across the plasmapause.

Vasyliunas [1966] has speculated that resonant interaction with VLF waves would enhance electron precipitation. This charge inbalance would induce a steady state electric field along the field lines which

would draw up thermal ionospheric electrons to maintain charge neutrality. Such a mechanism would not necessarily affect the proton distribution and would be consistent with a constant number density across the inner edge of the plasma sheet. Furthermore it would explain the order of magnitude decrease in the 'temperature' of the plasma sheet electrons. For a further discussion of pitch angle scattering see Roberts [1969]. One implication of this pitch angle scattering mechanism is that the structure of the inner edge should be strongly dependent upon pitch angle. The plasma sheet should extend further earthward in measurements of equatorial electron intensities with $\alpha \simeq 90°$ as compared with high latitude electron intensities which must precipitate out quite rapidly in order to decrease the energy density. Figure 9 illustrates the differential flux across the inner edge of the plasma sheet measured at two different pitch angles. No radial dependence of electron flux on pitch angle is observed. This is not to say that pitch angle scattering is not occurring, only that it does not appear to be a dominant feature in forming the inner edge of the plamsa sheet.

A third possibility is that the inner edge of the plasma sheet is an Alfvén layer. In this case plasma sheet particles are convected into the dipolar magnetic field and are then deflected by the resultant gradient drift. See Schield et al., [1969] and the references therein for a review. This Alfvén mechanism would deflect higher energy particles at greater distances and could result in an inward decrease in

the number density of the convected plasma sheet particles. The associated charge separation would result in field-aligned currents which consist mainly of ~ 100-eV electrons [Schield, 1968]. Although the Alfvén Layer theory is consistent with the observations of the structure of the inner edge it has further implications which remain unchecked (such as the simultaneous deflection of protons). However the relatively constant separation between the locations of the plasmapause and the inner edge of the plasma sheet is an indication that a common mechanism is involved.

Comparison with Other Observations. In general, earlier observations of the plasma sheet are in fair agreement with those presented here. Peak integral electron fluxes above 200 eV of $\sim 2 \times 10^8$ $(cm^2\text{-sec})^{-1}$ over a hemisphere were measured on board Lunik 1. The integral electron fluxes of $\sim 10^{10}$ $(cm^2\text{-sec})^{-1}$ measured with OGO-3 exceeded these by about an order of magnitude. Freeman [1964] noted that the electron flux would be $\sim 10^9$ $(cm^2\text{-sec-sr})^{-1}$ if the observed energy flux were produced by 10 keV electrons. This equivalent energy flux of 16 ergs$(cm^2\text{-sec-sr})^{-1}$ is within a factor of two of those presented here. The OGO-3 measurements of the plasma sheet within 12 R_E indicate the average electron energy, $\overline{E} = (U_e/n_e)$, is ~ 3-5 keV although the energy of the peak differential intensities occurs at ~ 1 keV.

The ATS low-energy detector observed particle fluxes of $.3-2 \times 10^7$ $(cm^2\text{-sec-sr})^{-1}$ at 6.6 R_E. Particles observed include electrons above 3 keV and all protons [Freeman and Maguire, 1967]. On June 23, 1966, inbound at L = 6.6 R_E at local midnight OGO-3 observations indicate the integral electron flux in the inner edge of the plasma sheet above 3 keV was 3.2×10^8 $(cm^2\text{-sec-sr})^{-1}$, a factor of twenty greater than the integral proton flux above 100 eV. Although the efficiencies of the ATS low-energy detector for both electrons and protons have not been published, Frank [1965] and Frank et. al., [1969] have shown that the Channeltron efficiency in counting 3 keV electrons is ~ 20 to 40% of the efficiency in counting protons between 3 and 30 keV. Even so, on June 23 the electron flux would have produced at least 80% of the counts in such a detector. On July 19 at L = 6.6 R_E the electron flux in the electron trough above 3 keV was 2.8×10^7 $(cm^2\text{-sec-sr})^{-1}$, about 80% of the proton flux above 100 eV. The protons would produce at least 75% of the counts in such a detector. Even if the calibration of this instrumentation were available the identification of the plasma component observed by the ATS low-energy detector above 50 eV in this environment would probably remain impossible.

Although Vasyliunas' [1968] main conclusions are substantiated his observation of the inner edge at 11 ± 1 R_E was not. The differences

in the location of this inner edge may be entirely latitude and local time differences between the measurements. OGO-3 observations of the inner edge at $L \simeq 15°$ near local midnight could map onto an equatorial crossing radius of $\sim 10\ R_E$. Furthermore Vasyliunas' quiet time observations were made between 1700 and 2100 LT whereas these OGO-3 measurements were made between 2100 and 0100 LT. Analysis of subsequent OGO-3 data should clarify this difference.

Acknowledgements

We would like to thank H. A. Taylor of the Goddard Space Flight Center for providing plasmapause locations observed with his ion spectrometer. This research was supported in part by the National Aeronautics and Space Administration under grant NsG-233-62 and contract NAS5-2054 and by the Office of Naval Research under contract Nonr-1509(06).

References

Carpenter, D. L., Whistler studies of the plasmapause in the magnetosphere, J. Geophys. Res., 71, 693-709, 1966.

Frank, L. A., Low-energy proton and electron experiment for the orbiting Geophysical Observatories B and E, U. of Iowa Res. Rep. 65-22, July, 1965.

Frank, L. A., Initial observations of low-energy electrons in the earth's magnetosphere with OGO 3, J. Geophys. Res., 72, 185-195, 1967a.

Frank, L. A., Several observations of low-energy protons and electrons in the earth's magnetosphere with OGO 3, J. Geophys. Res., 72, 1905-1916, 1967b.

Frank, L. A., On the extraterrestrial ring current during geomagnetic storms, J. Geophys. Res., 72, 3753, 1967c.

Frank, L. A., Recent observations of low-energy charged particles in the earth's magnetosphere, Physics of the Magnetosphere, ed. by R. L. Carovillano, J. F. McClay and H. R. Radoski, D. Reidel Publishing Co., Dordrecht-Holland, 271-289, 1967d.

Frank, L. A., On the distribution of low-energy protons and electrons in the earth's magnetosphere, Earth's Particles and Fields, ed. by B. M. McCormac, Reinhold Book Co., New York, 57-87, 1968.

Frank, L. A., N. K. Henderson and R. L. Swisher, Degradation of continuous-channel electron multipliers in a laboratory operating environment, Rev. Sci. Instr., 40, 685, 1969.

Freeman, J. W., Jr., The morphology of the electron distribution in the outer radiation zone and near the magnetospheric boundary as observed by Explorer 12, J. Geophys. Res., 69, 1691, 1964.

Freeman, J. W., Jr., and J. J. Maguire, Gross local-time particle asymmetries at the sychronous orbit altitude, J. Geophys. Res., 72, 5257, 1967.

Gringauz, K. A., Low energy plasma in the magnetosphere, Magnetospheric Physics, ed. by Williams and Mead, William Byrd Press, 339, 1969, and Rev. of Geophysics, 7, nos. 1 and 2, 1969.

Roberts, Charles S., Pitch-angle diffusion of electrons in the magnetosphere, in Magnetospheric Physics, ed. by Williams and Mead, William Byrd Press, 305, 1969, and Rev. of Geophysics, 7, nos. 1 and 2, 1969.

Schield, M. A., Configuration of geomagnetic field lines above the auroral zone, Ph.D. thesis, Rice University, Houston, Texas, 1968.

Schield, M. A., J. W. Freeman and A. J. Dessler, A source for field-aligned currents at auroral latitudes, J. Geophys. Res., 74, 247, 1969.

Swisher, R. L., and L. A. Frank, Lifetimes for low-energy protons in the outer radiation zone, J. Geophys. Res., 73, 5665, 1968.

Taylor, H. A., H. C. Brinton and M. W. Pharo, III, Contraction of the plasmasphere during geomagnetically disturbed periods, J. Geophys. Res., 73, 961, 1968.

Figure Captions

Figure 1. Dipole magnetic latitude and local time profiles for sample OGO-3 inbound orbits. The local time profile shifts westward by $\sim 1°$ per day. Although the inbound spacecraft is at low latitudes, with $\lambda_d \leq 25°$ within 15 R_E, the orbit cannot necessarily be described as near-equatorial beyond 8 R_E. An anti-solar neutral sheet hinged to the dipole equatorial plane at 10 R_E would lie within the indicated sectors.

Figure 2. Differential electron intensities across the inner edge of the plasma sheet and into the plasmasphere. During this pass the inner edge of the plasma sheet is located inside the boundary of trapping based on the response of the thin-windowed 213A GM tube as a function of the magnetic shell parameter L. The near-earth decrease in electron flux occurs at increasing radial distances for higher electron energies. The plasmapause is encountered within 1.5 R_E of the inner edge of the plasma sheet. The differential fluxes above 1 keV are continuous across this boundary. The existence of a plasmapause structure of less than 0.5 R_E is indicated by the localized increase in the electron fluxes below 750 eV.

Figure 3. Electron number and energy density across the inner edge of the plasma sheet and into the plasmasphere. The energy density decreased exponentially by an order of magnitude over 1.2 R_E with a scale length of one-third an earth radii. Initially this decrease was produced by a decrease in the higher energy electron fluxes (tens of keV) without decreasing the electron number density appreciably. Ultimately the decrease in energy density was produced almost entirely by a decrease in the keV fluxes. A constant number density above 90 eV was maintained by the simultaneous appearance of ~ 100-eV electrons. Note that the plasmapause was located at the minimum of the energy density profile for the fluxes above 750 eV.

Figure 4. Differential electron spectrums across the inner edge of the plasma sheet and the plasmapause. Initially the higher energy flux decreases between spectrums 1b and 2a followed by a decrease in the keV flux between spectrums 2a and 2b. Spectrum 2b illustrates the low energy portion of the electron flux in the electron trough. The plasmapause spectrum 3a quickly decreases to a typical plasmasphere spectrum 3b.

Figure 5. Count rate data are shown for two successive frames from detectors A and B. Data is telemetered every second for 19 seconds from each energy channel in succession. The counts for the 06:17 frame (dashed lines) for channels 4-8 are due mainly to scattered keV electrons. The 06:22 data generally follows that of the previous frame until an abrupt change occurs at 18 seconds, marked by the vertical dashed line. The shaede areas represent the difference between the observed count rate and the average counting rate in the following frame.

Figure 6. Radial profile of the energy and number density and average energy for electrons ($E \geq 90$ eV) near 22:00 LT. The average energy is the energy density divided by the number density for all observed electrons. The electron trough of ~ 100-eV electrons is easily discernable between the inner edge of the plasma sheet and plasmapause. The smooth transistion into the plasmasphere may be associated with the high fluxes inside the plasmasphere which were trapped during the July 9 storm. (See Figure 8).

Figure 7. Differential electron spectrums from the plasma sheet, the inner edge, the electron trough and the plasmasphere. The electron trough spectrum should peak near ~ 100 eV in order to maintain charge neutrality with the observed proton densities of ~ 2-5 $(cm)^{-3}$ above 100 eV.

Figure 8. Radial profile of electron energy density for $L \leq 10\ R_E$. An inbound measurement was made every orbital period (~ 2 days). The location of the inner edge of the plasma sheet is identified by the rapid earthward decrease in the electron energy density. (On June 23 this occurs for L between 7.1 and 5.9 R_E. See Figure 3). The structure of the inner edge is illustrated by the horizontal 'error bars'. These bars designate the position of the earthward decrease from a maximum to a minimum in the flux measured by a given channel. Unless otherwise specified the bars above and below the horizontal column are for channels 10 and 8 respectively as illustrated for June 11. Normally the lower bar is displaced earthward from the upper bar indicating the tendency for the lower energy fluxes ($E \simeq 1$ keV) to decrease closer to the earth. The inward displacement of the plasmapause during magnetic storms is

clearly seen. The trough of low energy electrons is invariably located in the region of low energy density between the inner edge of the plasma sheet and the plasmapause.

Figure 9. Differential electron fluxes measured by two detectors with perpendicular fields-of-view, LEPEDEA's A and B, which receive electrons having dipole pitch angles of $\sim (180\text{-}65°)$ and $\sim 35°$ respectively. By definition α is zero if the particle velocity is parallel to the magnetic field vector B. Any symmetric inflation of the dipole field should increase both α_A and α_B thus decreasing the difference between the sines of their pitch angles. On July 27 at $L = 3.6\ R_E$ a cross-calibration of the detectors while viewing identical pitch angles indicates that there is less than a 30% difference in the responses of the two instruments. No dependence of the electron flux profile on pitch angle has been observed on the six inbound passes for which such an analysis has been performed.

A-G69-523

SAMPLE OGO-3 ORBITS, INBOUND

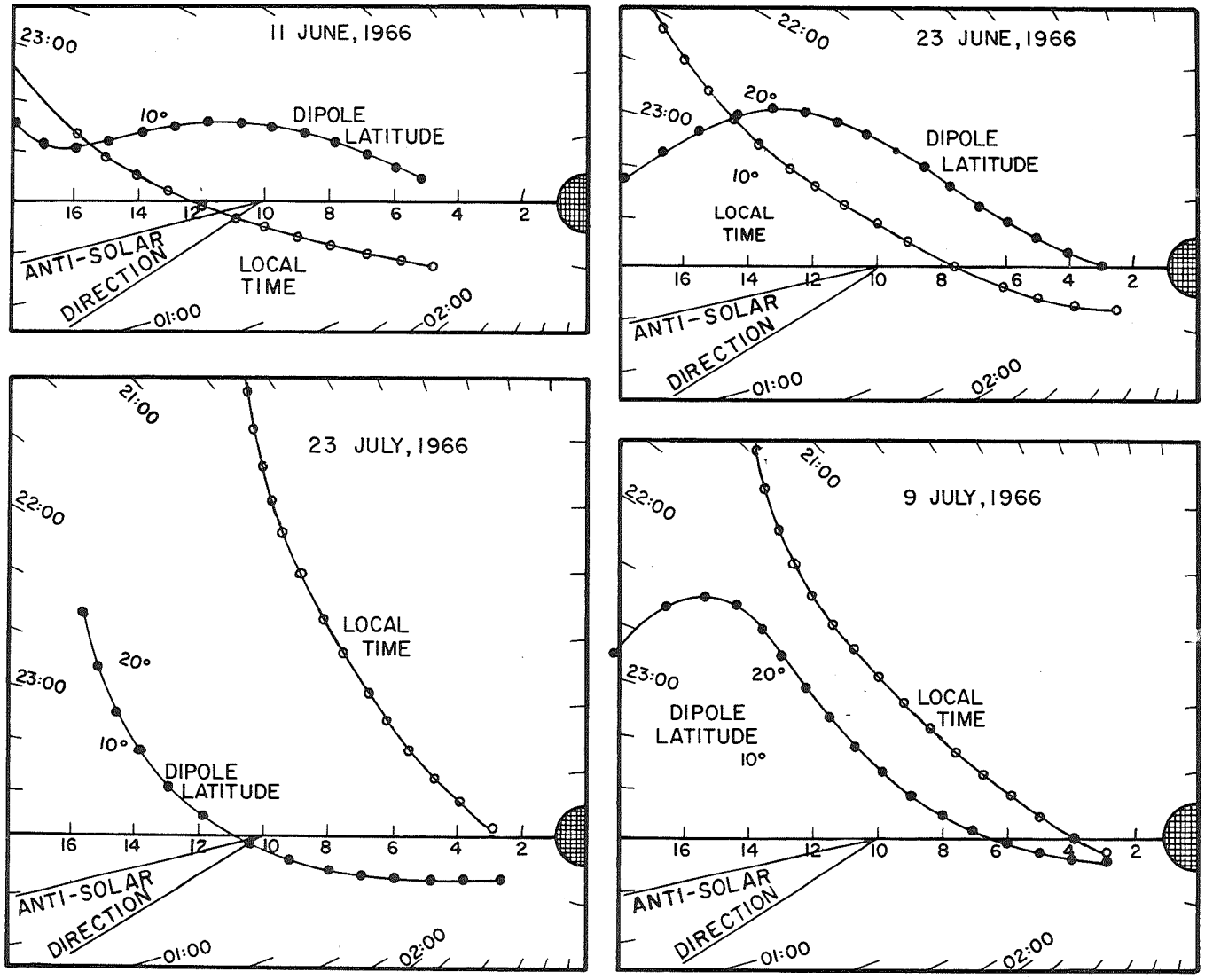

Figure 1

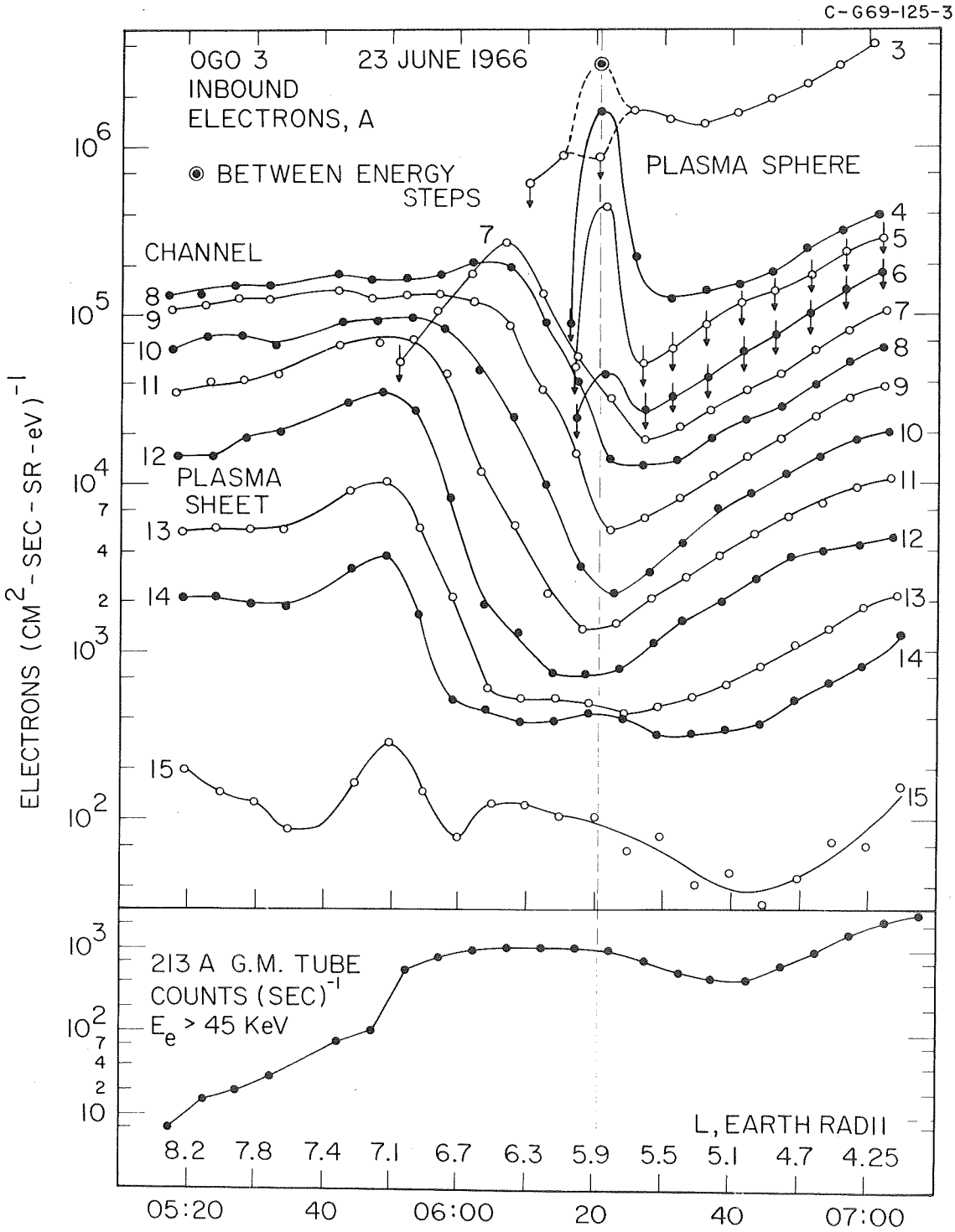
C-G69-125-3
OGO 3
23 JUNE 1966
INBOUND
ELECTRONS, A
BETWEEN ENERGY STEPS
PLASMA SPHERE
CHANNEL
PLASMA SHEET
ELECTRONS (CM^2-SEC-SR-eV)$^{-1}$
213 A G.M. TUBE
COUNTS (SEC)$^{-1}$
E_e > 45 KeV
L, EARTH RADII
8.2 7.8 7.4 7.1 6.7 6.3 5.9 5.5 5.1 4.7 4.25
05:20 40 06:00 20 40 07:00

Figure 2

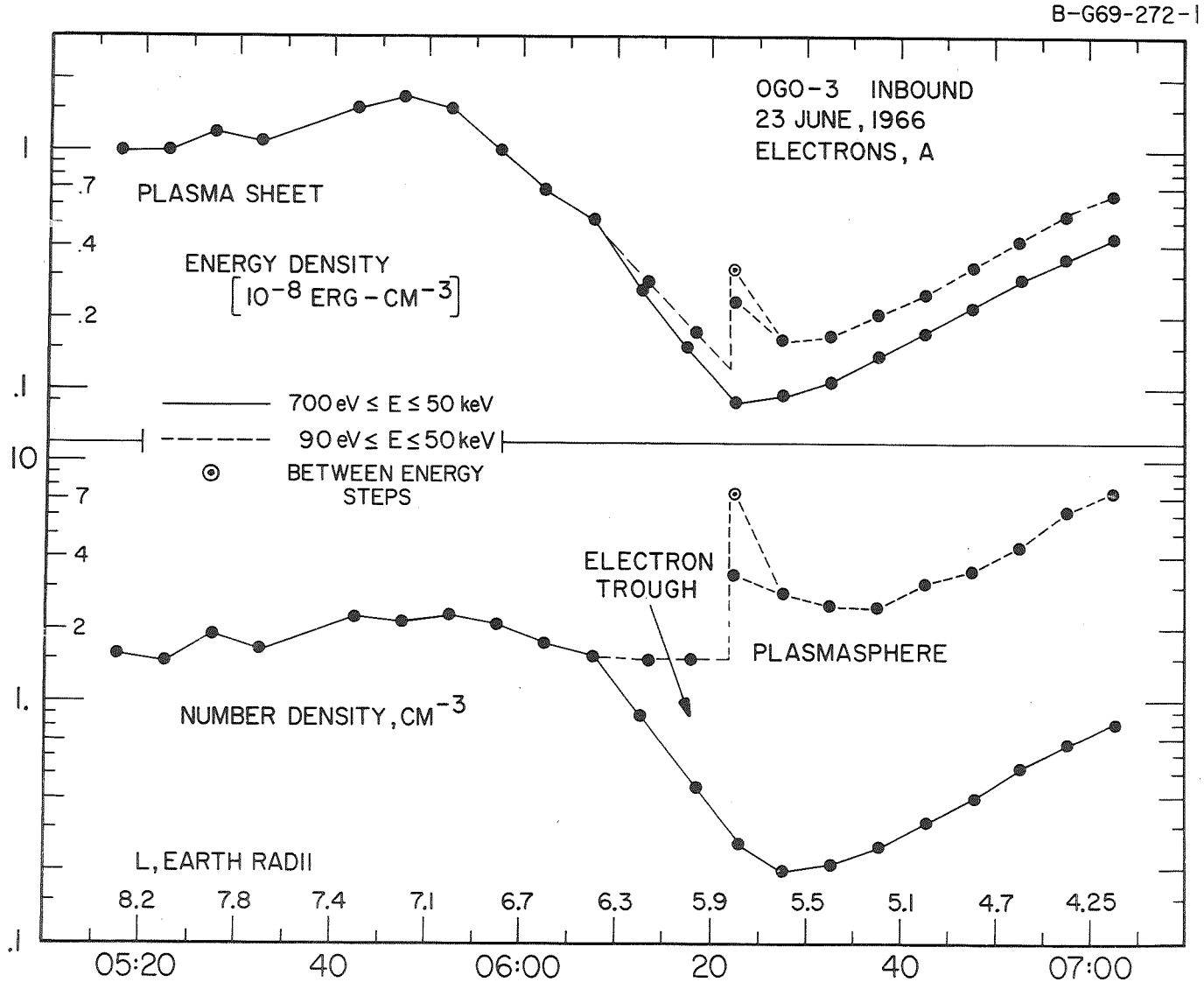
B-G69-272-1
OGO-3 INBOUND
23 JUNE, 1966
ELECTRONS, A
PLASMA SHEET
ENERGY DENSITY
[10^-8 ERG-CM^-3]
700 eV ≤ E ≤ 50 keV
90 eV ≤ E ≤ 50 keV
BETWEEN ENERGY STEPS
ELECTRON TROUGH
PLASMASPHERE
NUMBER DENSITY, CM^-3
L, EARTH RADII
8.2
7.8
7.4
7.1
6.7
6.3
5.9
5.5
5.1
4.7
4.25
05:20
40
06:00
20
40
07:00

Figure 3

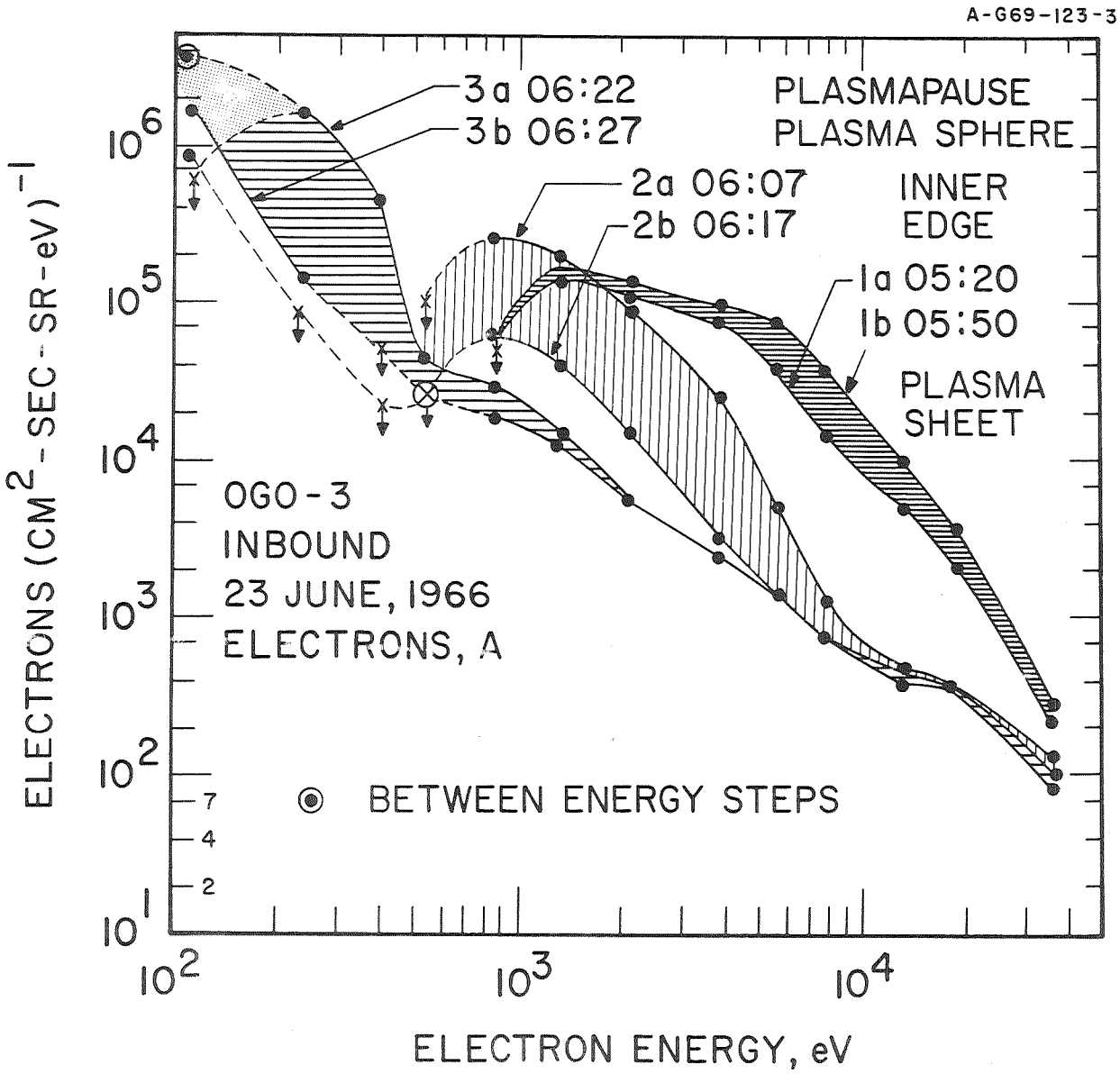
A-G69-123-3
3a 06:22
3b 06:27
PLASMAPAUSE
PLASMA SPHERE
2a 06:07
2b 06:17
INNER
EDGE
1a 05:20
1b 05:50
PLASMA
SHEET
OGO-3
INBOUND
23 JUNE, 1966
ELECTRONS, A
BETWEEN ENERGY STEPS
ELECTRONS (CM^2-SEC-SR-eV)$^{-1}$
ELECTRON ENERGY, eV
10^6
10^5
10^4
10^3
10^2
10^1
7
4
2
10^2
10^3
10^4

Figure 4

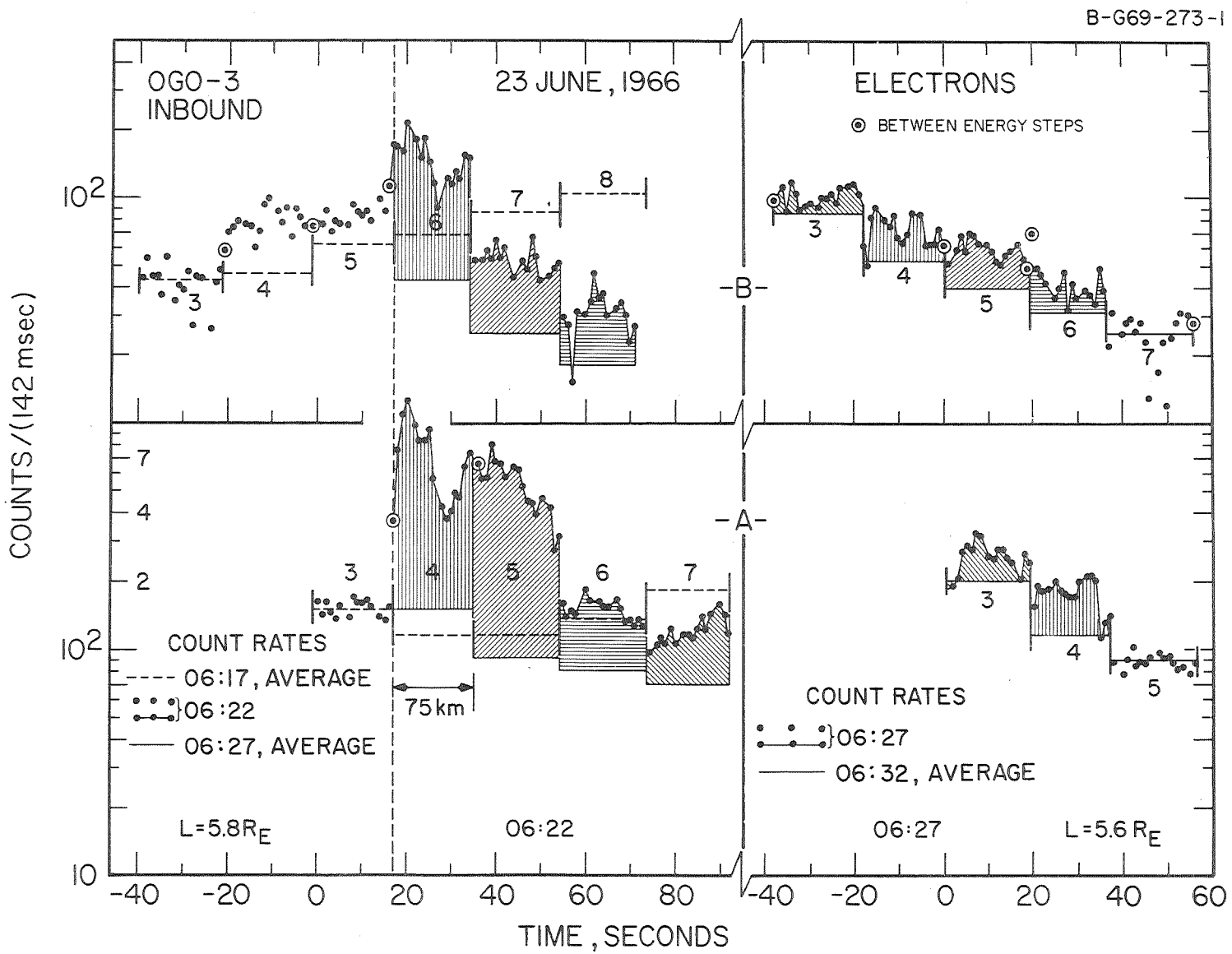
B-G69-273-1
OGO-3
INBOUND
23 JUNE, 1966
ELECTRONS
BETWEEN ENERGY STEPS
-B-
-A-
COUNTS/(142 msec)
COUNT RATES
06:17, AVERAGE
06:22
06:27, AVERAGE
75 km
L=5.8R_E
06:22
COUNT RATES
06:27
06:32, AVERAGE
06:27
L=5.6 R_E
TIME, SECONDS

Figure 5

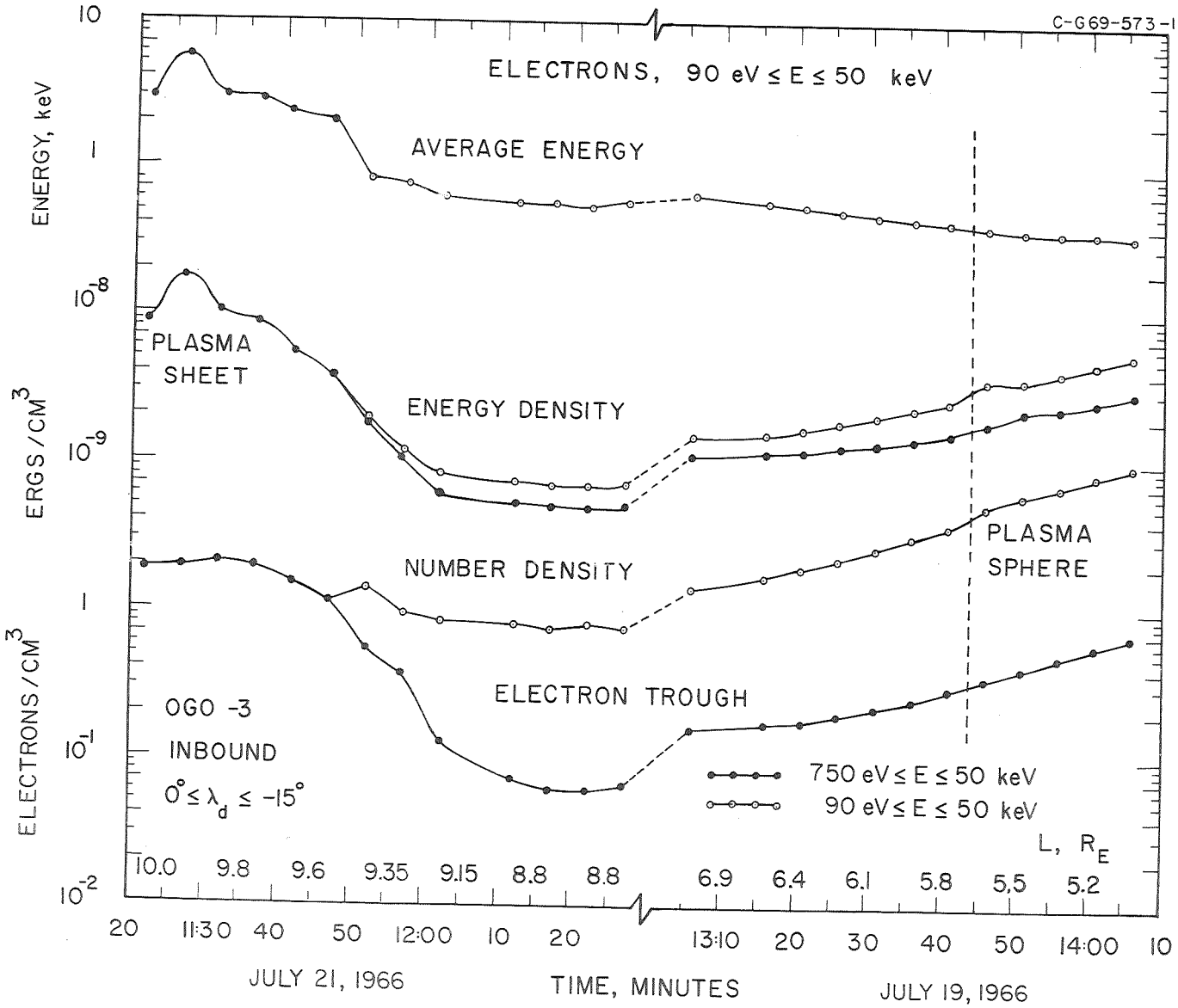
C-G69-573-1
ELECTRONS, 90 eV ≤ E ≤ 50 keV
AVERAGE ENERGY
ENERGY, keV
10
1
10^{-8}
PLASMA SHEET
ENERGY DENSITY
ERGS/CM^3
10^{-9}
NUMBER DENSITY
PLASMA SPHERE
1
ELECTRON TROUGH
ELECTRONS/CM^3
10^{1}
OGO -3
INBOUND
$0° \leq \lambda_d \leq -15°$
750 eV ≤ E ≤ 50 keV
90 eV ≤ E ≤ 50 keV
L, R_E
10^{-2}
10.0 9.8 9.6 9.35 9.15 8.8 8.8 6.9 6.4 6.1 5.8 5.5 5.2
20 11:30 40 50 12:00 10 20 13:10 20 30 40 50 14:00 10
JULY 21, 1966
TIME, MINUTES
JULY 19, 1966

Figure 6

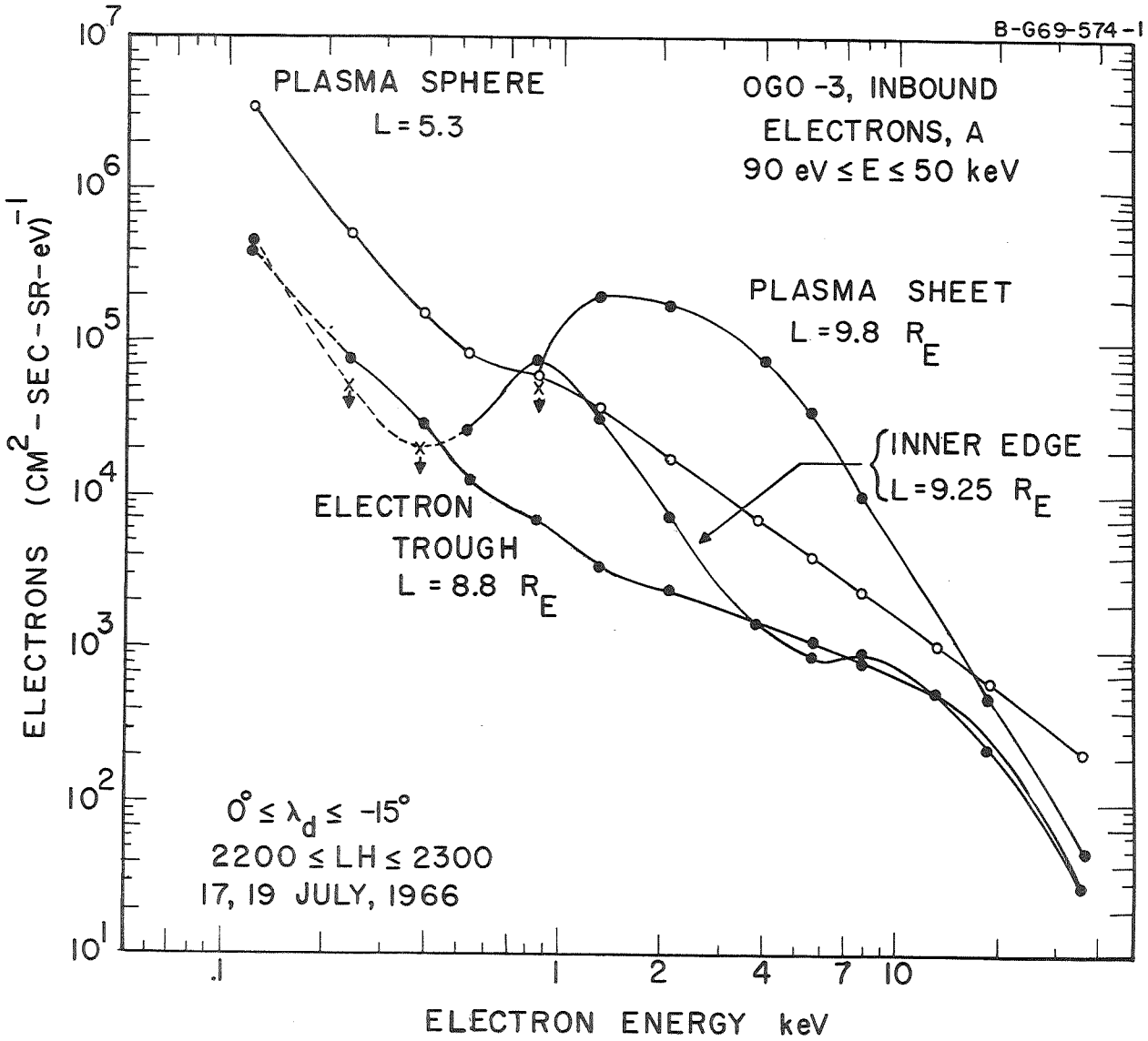
B-G69-574-1
PLASMA SPHERE
L = 5.3
OGO -3, INBOUND
ELECTRONS, A
90 eV ≤ E ≤ 50 keV
PLASMA SHEET
L = 9.8 R_E
INNER EDGE
L = 9.25 R_E
ELECTRON
TROUGH
L = 8.8 R_E
0° ≤ λ_d ≤ -15°
2200 ≤ LH ≤ 2300
17, 19 JULY, 1966
ELECTRONS (CM^2-SEC-SR-eV)^-1
ELECTRON ENERGY keV
10^7
10^6
10^5
10^4
10^3
10^2
10^1
.1
1
2
4
7
10

Figure 7

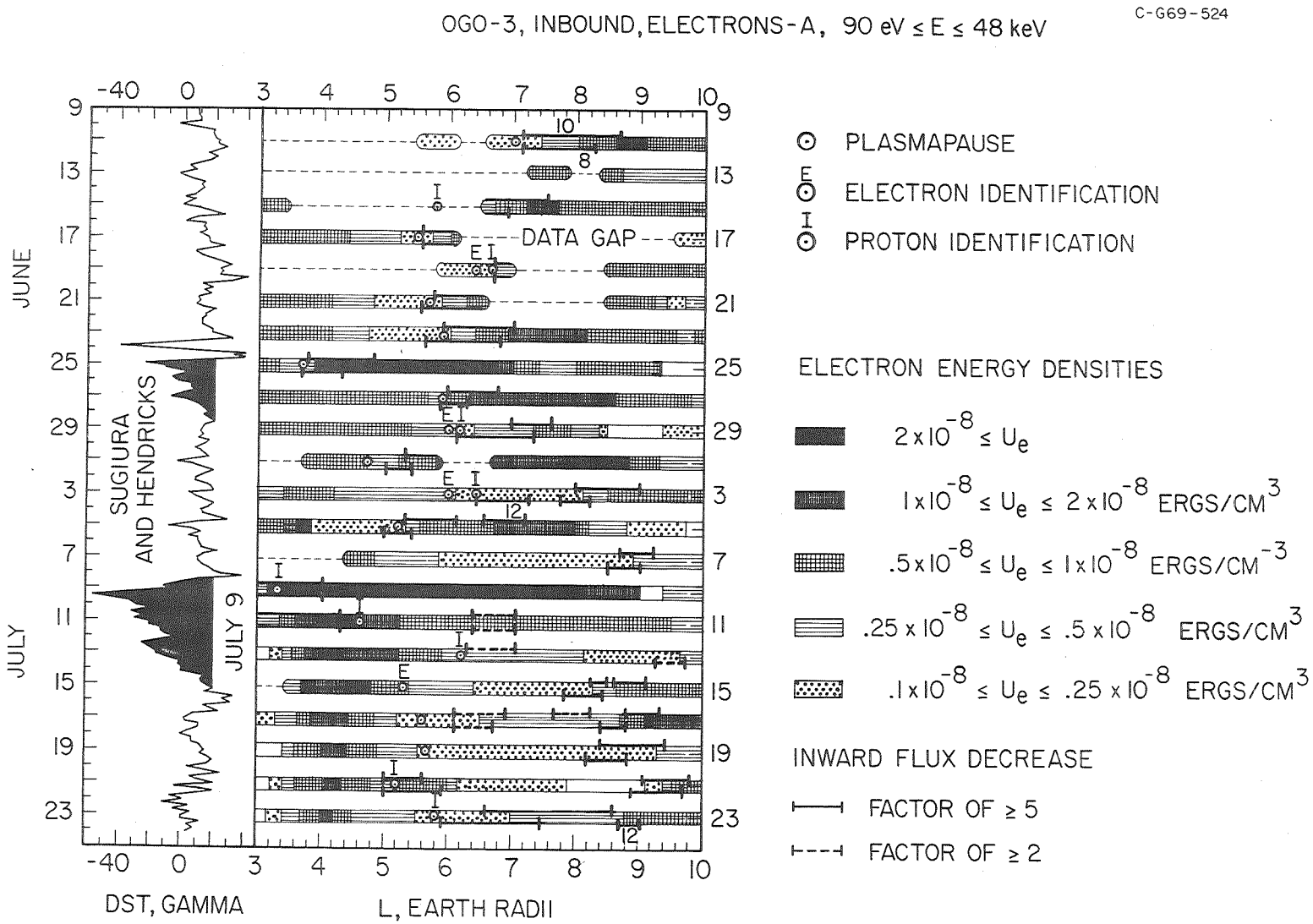
OGO-3, INBOUND, ELECTRONS-A, 90 eV ≤ E ≤ 48 keV
C-G69-524
JUNE
JULY
SUGIURA AND HENDRICKS
JULY 9
DATA GAP
DST, GAMMA
L, EARTH RADII
PLASMAPAUSE
ELECTRON IDENTIFICATION
PROTON IDENTIFICATION
ELECTRON ENERGY DENSITIES
2 x 10^-8 ≤ U_e
1 x 10^-8 ≤ U_e ≤ 2 x 10^-8 ERGS/CM^3
.5 x 10^-8 ≤ U_e ≤ 1 x 10^-8 ERGS/CM^-3
.25 x 10^-8 ≤ U_e ≤ .5 x 10^-8 ERGS/CM^3
.1 x 10^-8 ≤ U_e ≤ .25 x 10^-8 ERGS/CM^3
INWARD FLUX DECREASE
FACTOR OF ≥ 5
FACTOR OF ≥ 2

Figure 8

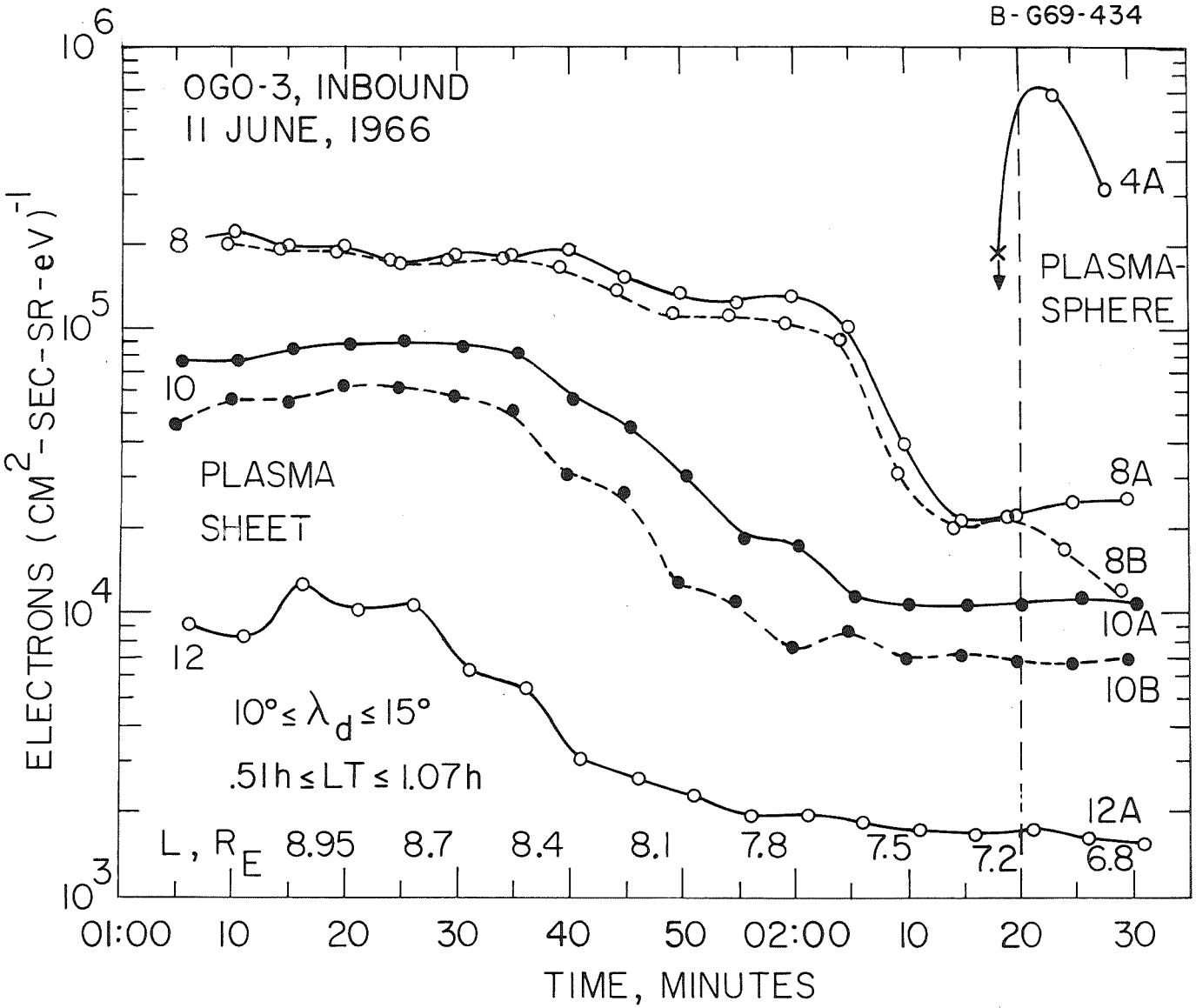
B-G69-434
OGO-3, INBOUND
11 JUNE, 1966
ELECTRONS (CM^2-SEC-SR-eV)$^{-1}$
10^6
10^5
10^4
10^3
8
10
12
PLASMA
SHEET
$10° \leq \lambda_d \leq 15°$
$.51h \leq LT \leq 1.07h$
L, R_E 8.95 8.7 8.4 8.1 7.8 7.5 7.2 6.8
4A
PLASMA-
SPHERE
8A
8B
10A
10B
12A
01:00 10 20 30 40 50 02:00 10 20 30
TIME, MINUTES

Figure 9

UNCLASSIFIED
Security Classification

DOCUMENT CONTROL DATA - R&D

(Security classification of title, body of abstract and indexing annotation must be entered when the overall report is classified)

1. ORIGINATING ACTIVITY *(Corporate author)* University of Iowa Department of Physics and Astronomy	2a. REPORT SECURITY CLASSIFICATION UNCLASSIFIED 2b. GROUP

3. REPORT TITLE

Electron Observations Between the Inner Edge of the Plasma Sheet and the Plasmasphere

4. DESCRIPTIVE NOTES *(Type of report and inclusive dates)*

Progress August 1969

5. AUTHOR(S) *(Last name, first name, initial)*

Schield, M. A. and Frank, L. A.

6. REPORT DATE August 1969	7a. TOTAL NO. OF PAGES 41	7b. NO. OF REFS 16
8a. CONTRACT OR GRANT NO. Nonr 1509(06) b. PROJECT NO. c. d.	9a. ORIGINATOR'S REPORT NUMBER(S) U. of Iowa 69-46 9b. OTHER REPORT NO(S) *(Any other numbers that may be assigned this report)*	

10. AVAILABILITY/LIMITATION NOTICES

Distribution of this document is unlimited.

11. SUPPLEMENTARY NOTES	12. SPONSORING MILITARY ACTIVITY Office of Naval Research

13. ABSTRACT

SEE PAGES FOLLOWING.

DD FORM 1 JAN 64 1473

UNCLASSIFIED
Security Classification

14. KEY WORDS	LINK A ROLE	LINK A WT	LINK B ROLE	LINK B WT	LINK C ROLE	LINK C WT
Radiation Zones						
Magnetic Storm						
Plasma Sheet						
Plasmasphere						
Plasmapause						

INSTRUCTIONS

1. ORIGINATING ACTIVITY: Enter the name and address of the contractor, subcontractor, grantee, Department of Defense activity or other organization *(corporate author)* issuing the report.

2a. REPORT SECURITY CLASSIFICATION: Enter the overall security classification of the report. Indicate whether "Restricted Data" is included. Marking is to be in accordance with appropriate security regulations.

2b. GROUP: Automatic downgrading is specified in DoD Directive 5200.10 and Armed Forces Industrial Manual. Enter the group number. Also, when applicable, show that optional markings have been used for Group 3 and Group 4 as authorized.

3. REPORT TITLE: Enter the complete report title in all capital letters. Titles in all cases should be unclassified. If a meaningful title cannot be selected without classification, show title classification in all capitals in parenthesis immediately following the title.

4. DESCRIPTIVE NOTES: If appropriate, enter the type of report, e.g., interim, progress, summary, annual, or final. Give the inclusive dates when a specific reporting period is covered.

5. AUTHOR(S): Enter the name(s) of author(s) as shown on or in the report. Enter last name, first name, middle initial. If military, show rank and branch of service. The name of the principal author is an absolute minimum requirement.

6. REPORT DATE: Enter the date of the report as day, month, year; or month, year. If more than one date appears on the report, use date of publication.

7a. TOTAL NUMBER OF PAGES: The total page count should follow normal pagination procedures, i.e., enter the number of pages containing information.

7b. NUMBER OF REFERENCES: Enter the total number of references cited in the report.

8a. CONTRACT OR GRANT NUMBER: If appropriate, enter the applicable number of the contract or grant under which the report was written.

8b, 8c, & 8d. PROJECT NUMBER: Enter the appropriate military department identification, such as project number, subproject number, system numbers, task number, etc.

9a. ORIGINATOR'S REPORT NUMBER(S): Enter the official report number by which the document will be identified and controlled by the originating activity. This number must be unique to this report.

9b. OTHER REPORT NUMBER(S): If the report has been assigned any other report numbers *(either by the originator or by the sponsor)*, also enter this number(s).

10. AVAILABILITY/LIMITATION NOTICES: Enter any limitations on further dissemination of the report, other than those imposed by security classification, using standard statements such as:

(1) "Qualified requesters may obtain copies of this report from DDC."

(2) "Foreign announcement and dissemination of this report by DDC is not authorized."

(3) "U. S. Government agencies may obtain copies of this report directly from DDC. Other qualified DDC users shall request through _____."

(4) "U. S. military agencies may obtain copies of this report directly from DDC. Other qualified users shall request through _____."

(5) "All distribution of this report is controlled. Qualified DDC users shall request through _____."

If the report has been furnished to the Office of Technical Services, Department of Commerce, for sale to the public, indicate this fact and enter the price, if known.

11. SUPPLEMENTARY NOTES: Use for additional explanatory notes.

12. SPONSORING MILITARY ACTIVITY: Enter the name of the departmental project office or laboratory sponsoring *(paying for)* the research and development. Include address.

13. ABSTRACT: Enter an abstract giving a brief and factual summary of the document indicative of the report, even though it may also appear elsewhere in the body of the technical report. If additional space is required, a continuation sheet shall be attached.

It is highly desirable that the abstract of classified reports be unclassified. Each paragraph of the abstract shall end with an indication of the military security classification of the information in the paragraph, represented as *(TS)*, *(S)*, *(C)*, or *(U)*.

There is no limitation on the length of the abstract. However, the suggested length is from 150 to 225 words.

14. KEY WORDS: Key words are technically meaningful terms or short phrases that characterize a report and may be used as index entries for cataloging the report. Key words must be selected so that no security classification is required. Identifiers, such as equipment model designation, trade name, military project code name, geographic location, may be used as key words but will be followed by an indication of technical context. The assignment of links, roles, and weights is optional.